

Alexander V. Ryzhkov, Janelle M. Janish, Terry J. Schuur, Pengfei Zhang, and Kimberly L. Elmore
Cooperative Institute for Mesoscale Meteorological Studies, Norman, Oklahoma

1. INTRODUCTION

One of the important advantages of polarimetric weather radars is their ability to discriminate between different types of hydrometeor and non-hydrometeor radar scatterers. Using a fuzzy logic classification algorithm, polarimetric measurands are combined to provide an identification of various hydrometeor types, such as rain, hail, graupel, wet snow, dry snow, and ice crystals of different orientation. These meteorological scatterers can be easily distinguished from non-meteorological targets, such as insects, birds, land and sea clutter (Zrnich and Ryzhkov 1999, Vivekanandan et al 1999).

This study focuses on the issues particularly important for aviation safety such as detection of hail, freezing rain, birds, discrimination between weather radar echoes and the echoes from land and sea surfaces. Here we present results of target classification based on multiparameter data obtained with two S-band polarimetric radars. One belongs to the NOAA National Severe Storms Laboratory (NSSL), and the other to the National Center for Atmospheric Research (NCAR). The data were collected in central Oklahoma and the Pacific Northwest respectively.

2. DETECTION OF HAIL

In the Spring of 2001, a series of regular observations with the NSSL's Cimarron dual-polarization radar were conducted in order to demonstrate its classification capability at the National Weather Service Forecast Office in Norman, OK. The emphasis was on detection of hail, identification of ground clutter (including the echoes caused by anomalous propagation), migratory birds and their discrimination from the echoes produced by clouds and insects. Measured radar variables included radar reflectivity factor Z , differential reflectivity Z_{DR} , differential phase Φ_{DP} , and cross-correlation coefficient ρ_{hv} . Only the data from the lowest elevation tilt of 0.5° were used for automatic classification.

Figure 1 illustrates a hailstorm case that occurred on 6 May 2001. The top panel represents distribution of radar reflectivity at the elevation of 0.5° in the 40×40 km area centered on the NSSL location where simultaneous measurements of drop size distribution were made with the 2D-video disdrometer. Differential reflectivity Z_{DR} exhibits relatively low values in the major reflectivity core which indicate the presence of hail

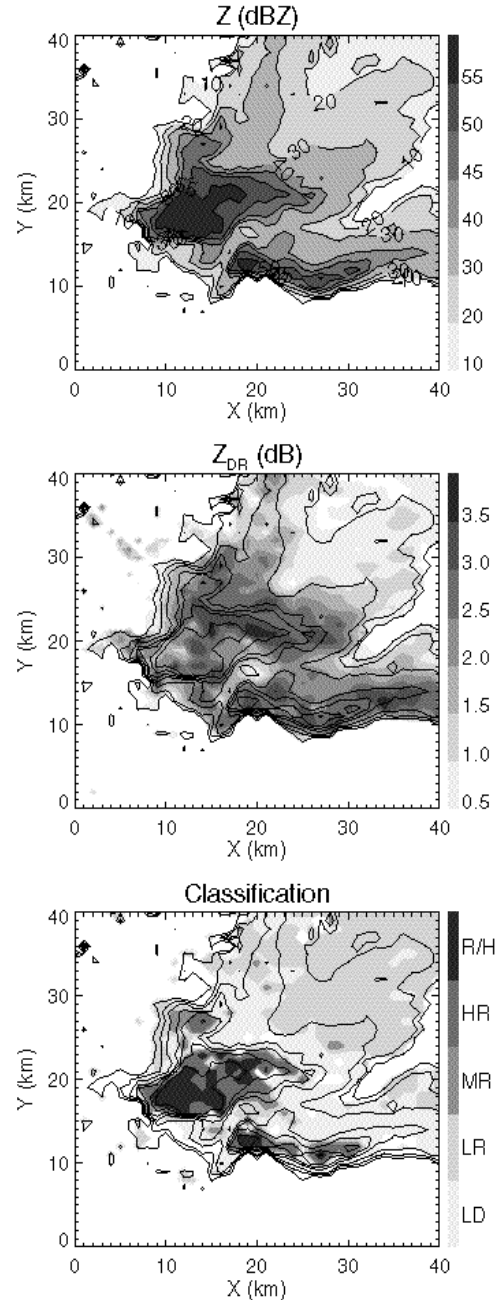


Fig.1 Fields of Z , Z_{DR} , and results of classification for the hailstorm of 6 May 2001 in Norman, OK. LD stands for 'large drops', LR – for light rain, MR – for moderate rain, HR – for heavy rain, R/H – for rain/hail mixture. Z contours are included on each panel

* Corresponding author address: Alexander V. Ryzhkov, CIMMS/NSSL, 1313 Halley Circle, Norman, OK 73069, e-mail: Alexander.Ryzhkov@noaa.gov

mixed with rain (R/H category in the classification plot). Note that extensive areas of radar echo are classified as “large drops”. This rain regime implies the presence of large drops combined with the deficit of small drops as can be confirmed from simultaneous measurements of drop size distributions performed with the 2D-video disdrometer (Fig. 2). The disdrometer is located at the center of the area displayed in Fig. 1. The instrument has caught several hailstones at about 20.8 UTC and

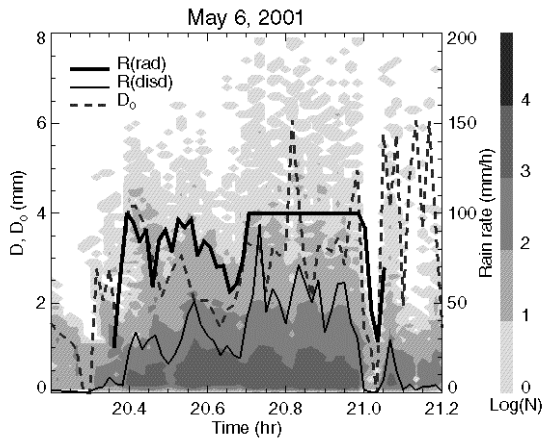


Fig.2 Time series of 1-min-averaged DSD, median volume diameter of raindrops D_0 , and rain rates R obtained from the disdrometer and the radar. Different shades are used to depict concentrations of drops for each size D in a logarithmic scale.

recorded plenty of giant drops with sizes between 6 and 8 mm that likely originated from melting hail and had ice cores inside. Domination of large drops in the spectrum leads to substantial overestimation of rainfall by a radar if conventional $R(Z)$ relation is used.

3. IDENTIFICATION OF INSECTS, BIRDS, AND AP.

Both migratory and roosting birds can pose serious threats to aviation. Very often insects and birds produce quite similar signatures in terms of radar reflectivity, Doppler velocity, and Doppler spectrum width. However, polarimetric variable Z_{DR} and Φ_{DP} allow us to distinguish between birds and insects almost unambiguously.

The night after a hailstorm hit central Oklahoma on 6 May 2001, extensive clear-air echo started building up (Fig. 3). This relatively weak echo was mixed with the echoes associated with a localized convective storm NE of the radar and anomalous propagation (AP) to the west of the radar. The sources of these radar echoes are easily recognized from the three polarimetric variables: Z_{DR} , Φ_{DP} , and ρ_{hv} . The convective storm is characterized by high values of ρ_{hv} and small values of Z_{DR} , whereas AP is identified by low ρ_{hv} and very noisy Z_{DR} and Φ_{DP} . Weaker background echo from migratory birds exhibits strong azimuthal dependence of differential reflectivity and differential phase. Both Z_{DR} and Φ_{DP} are much higher in the directions perpendicular to the direction of the birds' flight (from S to N). Maximal values of Z_{DR} and Φ_{DP} for birds in these directions (up to

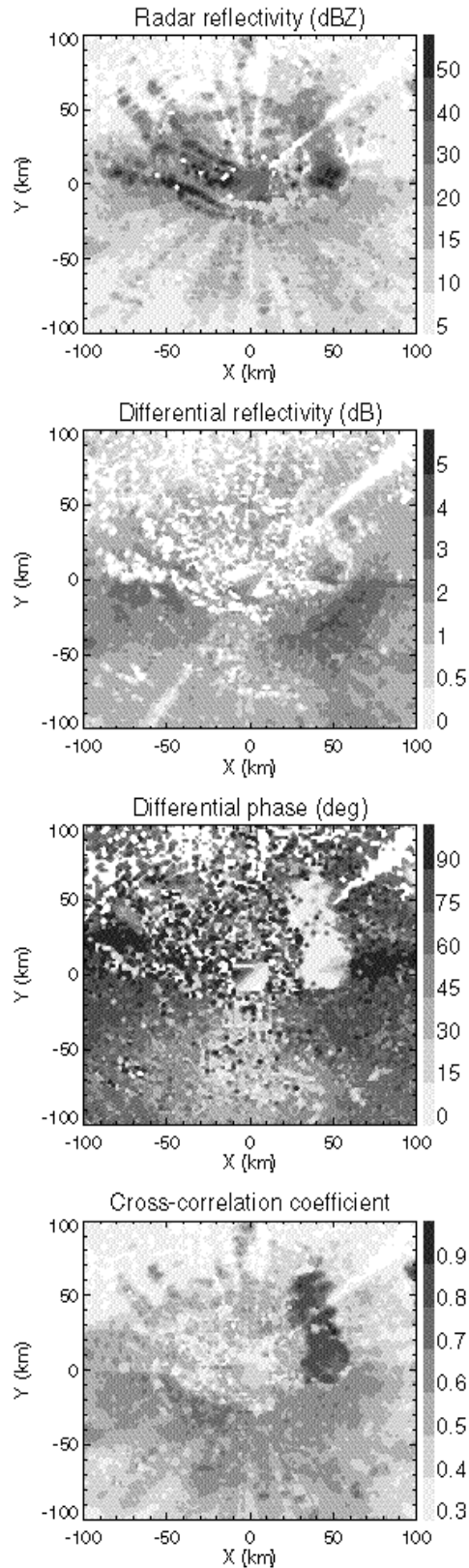


Fig. 3 Fields of Z , Z_{DR} , Φ_{DP} , and ρ_{hv} at the lowest elevation tilt (0.5°) for the case with birds, convective precipitation, and AP (05/07/01 04:11 UTC)

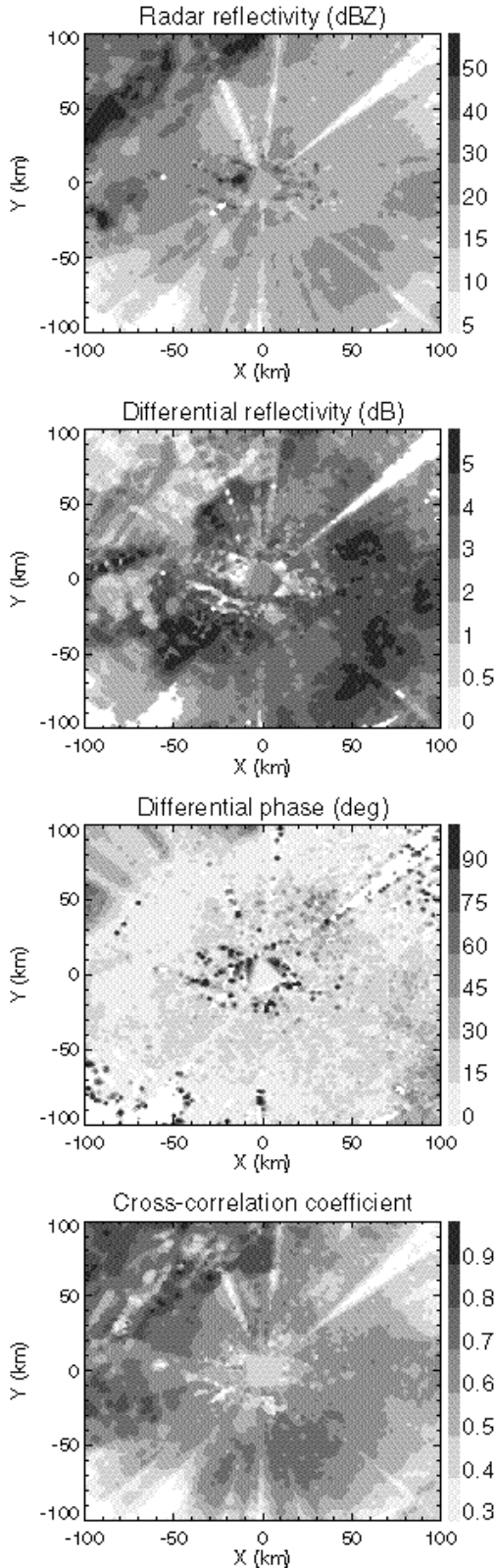


Fig. 4 Fields of Z , Z_{DR} , Φ_{DP} , and ρ_{hv} at the lowest elevation tilt (0.5°) for the case with insects and convective precipitation (05/30/01 02:00 UTC)

4 dB and 100° respectively) are much higher than for meteorological scatterers

Reflections from insects are characterized by much higher maximal values of Z_{DR} (up to 10 dB) and significantly lower maximal values of Φ_{DP} that do not exceed $20 - 30^\circ$ (Fig. 4). Using cross-correlation coefficient only, we can easily filter out radar echoes caused by biological scatterers or AP from weather echoes, but cannot distinguish between insects and birds. This distinction can be made by using maximal values of Z_{DR} and Φ_{DP} or by examination of azimuthal patterns of these two polarimetric variables.

4. DISCRIMINATION BETWEEN LIGHT RAIN, FREEZING RAIN, AND SNOW.

Freezing rain is a dangerous phenomenon for all kinds of traffic and transportation including air traffic in the terminal area of airports. In order to assess capability of a dual-polarization radar to identify freezing rain, we examined four recent winter events in Oklahoma. These include two cases of snow (11/28/01 and 02/05/02), one ordinary stratiform rain event (01/05/02), and one case of freezing rain (01/31/02) that resulted in approximately one hundred fifty million dollars damage in Oklahoma. Our analysis shows that the primary difference between these four storms is in differential reflectivity Z_{DR} and its dependence on radar reflectivity factor Z . Differential reflectivity is close to zero for aggregated snow near the ground regardless of its reflectivity, whereas Z_{DR} for rain is positive and increases with increasing Z (Fig. 5). The $Z - Z_{DR}$ pairs

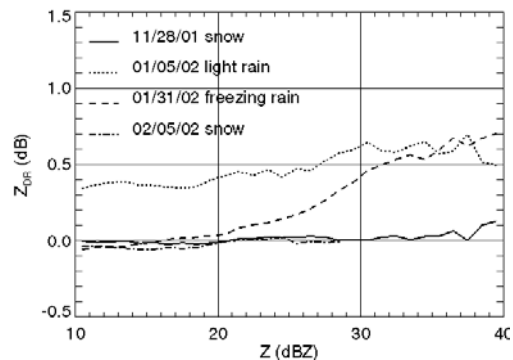


Fig. 5 Average dependencies of Z_{DR} on Z for four winter events.

were taken from the NW quadrant (where the largest damage from icing was documented) at lowest elevation tilt (0.5°). The mean values of Z_{DR} were calculated for each 1dB reflectivity bin. We restricted ourselves to ranges less than 100 km from the radar to avoid including too much data from upper levels. Fig. 5 shows that reliable distinction between rain and snow can be made only for reflectivities over 30 dBZ.

Although a dual-polarization radar enables discrimination between snow and rain, an analysis of surface temperature and sounding is necessary to delineate "ordinary rain" and freezing rain. Fig. 6

illustrates typical vertical profiles of temperature for all four cases. The freezing rain event is characterized

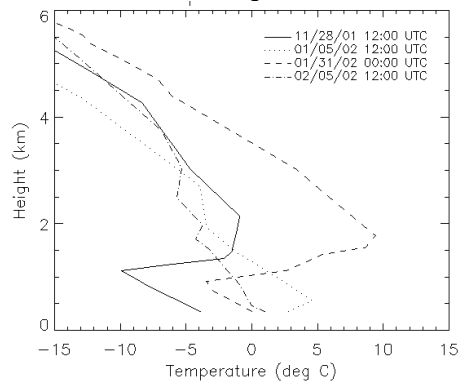


Fig. 6 Vertical profiles of temperature for four winter events (Norman location).

by a very strong temperature inversion aloft and by slightly negative surface temperatures. The sounding for this case (taken at Norman, OK, which was not hit by freezing rain) indicates the surface temperature about 0°C. In the zone of icing to the NW of Norman, surface temperatures were slightly negative (within the range from -3°C and -1°C). In contrast, no inversion was observed in the snow case of 02/05/02 and the surface temperature was slightly positive.

5. DISCRIMINATION BETWEEN SEA CLUTTER, MARINE STRATOCUMULUS, AND PRECIPITATION.

Marine stratus clouds in the vicinity of the approach zones of the airports in the Pacific Northwest region pose serious problem for FAA Traffic Management Coordinators. In the San Francisco International Airport, such clouds can prohibit dual approaches to the closely spaced parallel runways, thereby reducing airport capacity by half. Continuous radar monitoring of these low-level clouds is complicated by their low reflectivities (usually below 5 dBZ) and by the presence of backscatter from the sea surface. Sea clutter suppression in the frequency domain is not as efficient as land clutter suppression because the former has nonzero mean Doppler velocity.

We have examined polarimetric Doppler radar data obtained from the IMPROVE I Field Experiment: Offshore Frontal Precipitation Study conducted by the University of Washington west of the Seattle, WA, area during the period 4 January – 14 February 2001. The data were collected with the NCAR SPOL 10-cm dual-polarization radar located on the Pacific shoreline at the height of 10 m above sea level.

At least three types of radar echo are easily distinguishable: reflections from the sea surface, low-height marine stratocumulus clouds, and convective precipitation that is most often associated with atmospheric fronts. We developed classification schemes for pure Doppler radar and dual-polarization radar. Examples of classification for one of the days of observations are presented in Fig. 7.

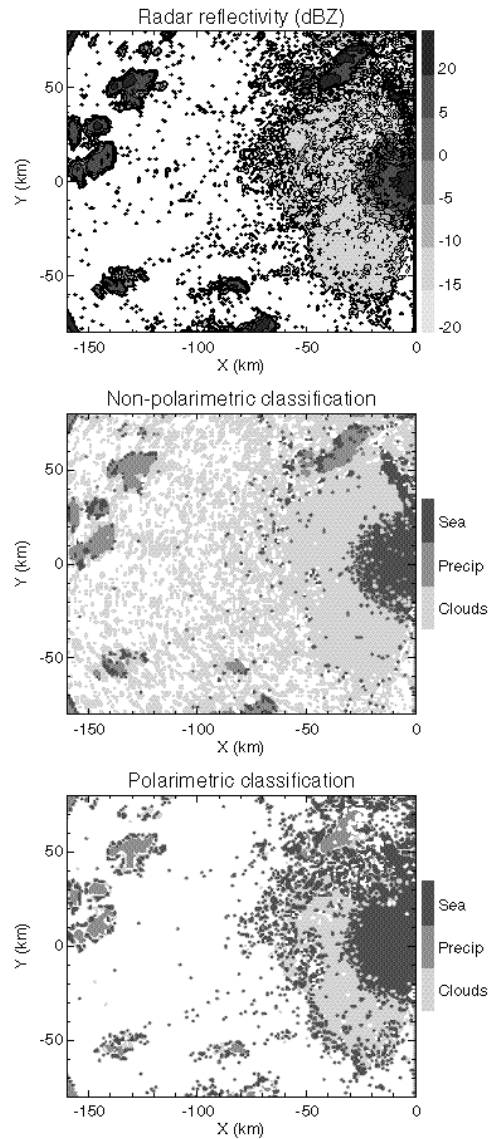


Fig. 7. Fields of Z and results of classification using non-polarimetric and polarimetric algorithms at the elevation of 0.0° in the marine sector on 02/02/01 16:10 UTC. The NCAR SPOL radar is located at (0,0).

Acknowledgement. The authors are thankful to Dr. C. Kessinger (NCAR) for providing SPOL data from the IMPROVE 1 Experiment.

References

Znic, D.S., and A.V. Ryzhkov, 1999: Polarimetry for weather surveillance radars. *Bull. Amer. Meteor. Soc.*, **80**, 389 – 406
 Vivekanandan, J., D.S. Znic, S.M. Ellis, R. Oye, A.V. Ryzhkov, and J. Straka, 1999: Cloud microphysics retrieval using S-band dual-polarization radar measurements. *Bull. Amer. Meteor. Soc.*, **80**, 381 – 388.